

A SIMPLE MODEL FOR THREE PHASE FLOW WITH HYSTERESIS*

A. J. de Souza D. Marchesin  P. Bedrikovetsky
P. Krause 

Abstract

We consider a model for a three phase flow in a reservoir, in an idealized situation where water and gas are miscible, but both are immiscible relative to oil. We assume that the hysteresis effects occur in the oil phase permeability only. This permeability varies irreversibly along two extreme curves (imbibition and drainage) bounding a region foliated by reversible permeability curves. We describe the structure of the fundamental waves and establish the existence of the Riemann solution.

Resumo

Neste trabalho consideramos um modelo de escoamento trifásico num reservatório petrolífero, numa situação idealizada onde as fases água e gás são consideradas miscíveis, porém ambas imiscíveis com relação à fase óleo. Supomos também que os efeitos de histerese ocorrem apenas na permeabilidade do óleo. Esta permeabilidade varia irreversivelmente ao longo de duas curvas extremas (embebimento e drenagem) delimitando uma região folheada por curvas de permeabilidade reversíveis. Finalmente, descrevemos a estrutura de ondas fundamentais e estabelecemos um teorema de existência para a solução do problema de Riemann.

1. Introduction

In this work we consider the Riemann problem for an idealized model of three phase flow (water/oil/gas) in porous media, taking into account hysteresis effects in the permeability of the oil phase. Hysteresis may be the most important phenomenon in multiphase flows lacking rigorous mathematical analysis in the literature.

*This work was supported in part by: CNPq under Grant 300204/83-3; CNPq under Grant 523258/95-0; FAPERJ under Grant E-26/150.936/99; FINEP under Grant 77.97.0315.00.

When capillary forces predominate, they determine the distribution of the several phases in the porous space.

If the distribution of phases over pore space at a certain time were unique and independent of the distribution at earlier times, then changes of any phase quantity would cause redistribution of the phases according to the rule described above, and physical properties such as relative permeabilities would depend only on saturations.

Unfortunately, this is not the case, and the past history of saturation in the porous medium affects strongly the current phase distributions.

We propose a model for the flow of three phases, which we call water, gas and oil. We assume that the hysteresis effects are expressed in the oil phase only. This model does not have a direct physical interpretation.

Mathematically, the hysteresis effects are modeled by assuming that there are two extreme permeability curves for the oil, called the imbibition and drainage curves, which describe the flow when oil saturation is decreasing and increasing, respectively, in an irreversible fashion. Within the extreme curves we assume that the oil permeability increases or decreases reversibly, following a family of permeability curves which foliates this region. These curves are called scanning curves. This model for two phase flow, proposed in [3, 4, 5] and further studied in [2], takes into account the extreme curves as well as the scanning curves. The independent variables are saturation and a hysteresis parameter for the family of scanning curves.

For two phase flow the first attempt to obtain a Riemann solution with hysteresis effects containing some of the features above was made in [6] and continued in [7]. In these papers only the two extreme imbibition and drainage permeability curves where the flow is irreversible were considered.

Our aim in this paper is to extend the technique applied in [2, 3, 4, 5] for two phase flow to the three phase flow model. Besides difficulties in the calculations, one of the main obstacles is understanding the fundamental wave structure in a three dimensional state space. As a first step towards understanding this geometry, in this work we consider a simple situation where the water and gas

permeability functions are taken to be linear while the oil permeability satisfies generic conditions, except for the scanning permeability curves, which give rise to contact waves by means of a simplification to avoid technicalities. With this simplification, we were able to obtain the complete structure of the elementary waves and to put them together to describe the Riemann solution. There are three kinds of elementary waves: stationary waves originating from the fact that the hysteresis parameter is time independent in the scanning region; contact scanning waves; and saturation waves corresponding to a Buckley-Leverett solution for a scalar conservation law obtained by combining the saturation equations in different regimes.

The paper is subdivided in six sections and an Appendix. The Appendix is independent; its purpose is to remind the reader of the Riemann solution construction for the *two* phase flow model with hysteresis effects [2, 3, 4, 5]. In Section 2, the Buckley-Leverett system for three phase flow without hysteresis is derived, based on the conservation of mass and on Darcy's law of force. In Section 3 the hysteresis parameter π is introduced in the equations obtained in Section 2 to obtain the three phase flow model with hysteresis. In this section the generic assumptions on the oil permeability curves are also stated. In Section 4 a *formalism for the extended flow functions* is introduced, preparing for the description of elementary waves and of the Riemann solution. Extended flow functions relate states in distinct flow regimes, drainage, imbibition and scanning. In Section 5 the model is analyzed. Linear water and gas permeability functions are employed. In the subsections of Section 5, wave resonance is discussed and the structure of the elementary waves is analyzed, comprising stationary waves, contact scanning waves and saturation waves. Each regime of the fluid is discussed; these regimes are connected by using extended flow functions. The Riemann solution based on the results of Section 5 is constructed in Section 6. It is shown that there are three possible wave sequences in the Riemann solution connecting a left state to a right state. The sequences always start by a stationary wave, which is followed by a contact or a saturation wave. The order of the latter two waves depends on the location of the left and right

states.

Thus our main result is the existence of the Riemann solution for all initial data.

2. The Buckley-Leverett System for Three-Phase Flow

We consider one-dimensional, horizontal flow of three fluid phases in a porous medium. We assume that a certain infinitesimal volume of reservoir at position x and time t has water saturation s_w , oil saturation s_o and gas saturation s_g .

The differences among these phases lie in some flow properties. We assume that the whole pore space is occupied by the fluid and that there are no sources or sinks. Compressibility, thermal and gravitational effects are neglected.

The equations expressing conservation of mass of water, gas, and oil are in one spatial dimension

$$\frac{\partial}{\partial t}(\phi s_\alpha \rho_\alpha) + \frac{\partial}{\partial x}(\rho_\alpha v_\alpha) = 0, \quad \alpha = w, g, o, \quad (2.1)$$

respectively, where ϕ denotes the porosity of the porous medium and for the phase α , ρ_α denotes the density and v_α is the seepage velocity (the product of the saturation by the particle velocity of the phase α). Since the fluid occupies the whole pore space, the saturations satisfy

$$\sum_{\alpha} s_\alpha = 1. \quad (2.2)$$

The theory of multiphase flow in porous media is based on the following form of Darcy's law of force [1, 8]:

$$v_\alpha = -K \lambda_\alpha \frac{\partial}{\partial x} p_\alpha, \quad \text{for } \alpha = w, g, o. \quad (2.3)$$

where K denotes the absolute permeability of the porous medium, λ_α is the mobility of phase α , and p_α is the pressure of phase α . The mobility is usually expressed as $\lambda_\alpha = k_\alpha / \mu_\alpha$, the ratio of the relative permeability k_α and the viscosity μ_α of phase α . In the discussion now, we assume that the pressures in the water, oil and gas are the same, that is $p_o = p_w = p_g = p$. This is the same

as neglecting capillary pressure effects among the fluids; this approximation is valid in special circumstances.

The porosity ϕ and absolute permeability K are associated to the rock; we will take them to be constant. Neglecting thermal effects and compressibility, μ_α and ρ_α are constant too, and we can rewrite (2.1) without ρ_α .

Let us denote the total mobility by

$$\lambda = \sum_{\alpha} \lambda_{\alpha} \quad (2.4)$$

and define the fractional flows by

$$f_{\alpha} = \lambda_{\alpha}/\lambda, \quad \text{for } \alpha = w, g, o. \quad (2.5)$$

Of course,

$$\sum_{\alpha} f_{\alpha} = 1. \quad (2.6)$$

Introducing the total seepage velocity $v = \sum_{\alpha} v_{\alpha}$ we can write that

$$v f_{\alpha} = v_{\alpha}. \quad (2.7)$$

Therefore, by (2.1) and (2.7), the equations governing the flow are

$$\frac{\partial}{\partial t}(\phi s_{\alpha}) + \frac{\partial}{\partial x}(v f_{\alpha}) = 0, \quad \text{for } \alpha = w, g, o. \quad (2.8)$$

Summing (2.1) on α we find $\frac{\partial}{\partial x} v = 0$, so that v is a function of t alone. Assuming that v never vanishes, it is possible to change the variable t so that v is constant. As v is nonzero, we can set $t = (\phi K/v^2)\tilde{t}$ and $x = (K/v)\tilde{x}$, thereby removing v , ϕ , and K from system (2.8). For simplicity of notation, we drop the tildes.

If we choose s_w and s_g as the dependent variables, the Buckley-Leverett system for three-phase flow may be written as:

$$\frac{\partial s_w}{\partial t} + \frac{\partial f_w(s_w, s_g)}{\partial x} = 0, \quad (2.9)$$

$$\frac{\partial s_g}{\partial t} + \frac{\partial f_g(s_w, s_g)}{\partial x} = 0.$$

3. Hysteretic Scanning Flow for Three Phases in Porous Media

In this model, we assume that the oil phase exhibits hysteresis phenomena in its permeability, while the water and gas phases do not. Thus the internal distribution of the three fluids in an infinitesimal volume, resulting from its past evolution, is described by the value of a parameter π , which is a hysteresis parameter. This is the case when the fluid mixture is in “scanning” mode.

In the “scanning” mode, in general, the corresponding expression for oil permeability k_o depends on both s_o and on the hysteresis parameter π , varying in some interval. See [2, 3, 4, 5]. Thus Darcy’s law for the seepage flow speed of oil may be written as:

$$v_o = -\frac{K}{\mu_o} k_o^S(s_o; \pi) \frac{\partial p}{\partial x} \quad (\text{scanning}). \quad (3.1)$$

where k_o^S is the oil relative permeability function in the scanning mode, represented in Fig. 3.2.

Equation (3.1) is valid in the “scanning” range of oil saturations, $s_o^I(\pi) < s_o < s_o^D(\pi)$, shown in Fig. 3.1, which will be discussed later. Let us start with circumstances such that the mixture of fluids is in a “scanning”, or reversible, state. If the saturation is changed, the value of π describing the fluid state stays fixed, and the oil permeability changes with saturation following the “scanning curve” determined by the initial configuration (see Fig. 3.1, with $\pi = \tau$).

Movement along the interior of a scanning curve is reversible. However, if the oil saturation increases too much, the internal configuration of the fluid changes. This takes place when the state reaches the intersection of the scanning curve with the rightmost curve in Fig. 3.1. This intersection occurs when $s_o = s_o^D(\pi)$.

As long as the oil saturation continues to increase in time, the oil permeability follows this rightmost curve. Since water (and/or gas) “drains” when oil saturation increases, this curve defines the drainage oil permeability function, denoted by $k_o^D(s_o)$, which also is represented in Fig. 3.2. Thus we have Darcy’s

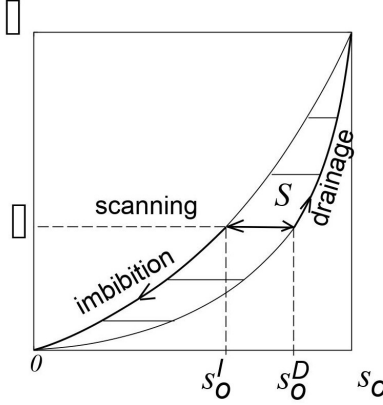


Figure 3.1: Imbibition, drainage and scanning curves in the space $(s_o; \pi)$.

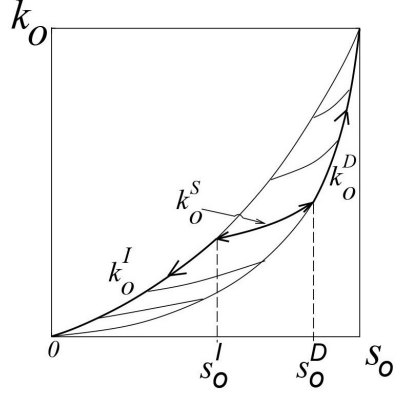


Figure 3.2: Permeability curves: oil, drainage and scanning family.

law

$$v_o = -\frac{K}{\mu_o} k_o^D(s_o) \frac{\partial p}{\partial x} \quad \text{if } s_o = s_o^D(\pi) \quad \text{and} \quad \frac{\partial s_o}{\partial t} > 0 \quad (\text{drainage}). \quad (3.2)$$

During drainage, the hysteresis parameter π changes. From the above discussion, it follows that this happens so that $s_o = s_o^D(\pi)$ is defined implicitly by

$$k_o^D(s_o) = k_o^S(s_o; \pi) \quad (\text{drainage}). \quad (3.3)$$

Similarly, after starting in a scanning mode, if the oil saturation decreases too much, the state reaches the intersection of the scanning curve with the leftmost curve in Fig. 3.1. This intersection occurs when $s_o = s_o^I(\pi)$.

As long as the oil saturation continues decreasing in time, the oil permeability follows this leftmost curve and defines the imbibition oil permeability function, denoted by $k_o^I(s_o)$, which also is represented in Fig. 3.2. We have

Darcy's law

$$v_o = -\frac{K}{\mu_o} k_o^I(s_o) \frac{\partial p}{\partial x} \quad \text{if } s_o = s_o^I(\pi) \quad \text{and} \quad \frac{\partial s_o}{\partial t} < 0 \quad (\text{imbibition}); \quad (3.4)$$

we also have that $s_o = s_o^I(\pi)$ is defined implicitly by

$$k_o^I(s_o) = k_o^S(s_o; \pi) \quad (\text{imbibition}). \quad (3.5)$$

Finally, when the fluid state is initially in drainage or in imbibition mode and then the oil saturation tendencies reverse sign the fluid goes back into a scanning mode. Only at the end states where the drainage and imbibition curves intersect the state can change directly between imbibition and drainage upon saturation tendency reversals.

In order to be more precise about the state space variables we will make the following assumptions keeping in mind the example $k_o(s_o) = s_o^2$ and the assumptions in [3, 4, 5]. Let \mathcal{S} be the closure of the scanning region in state space for variables s_o and π , defined as $\mathcal{S} = \{(s_o; \pi) \mid s_o^I(\pi) \leq s_o \leq s_o^D(\pi), 0 \leq \pi \leq 1\}$, see Fig. 3.1.

$$k_o^\alpha \in \mathcal{C}^2[0, 1], \quad \text{for } \alpha = D, I, \quad (3.6)$$

$$k_o^\alpha(0) = 0, \quad k_o^\alpha(1) = 1, \quad \frac{dk_o^\alpha}{ds_o}(0) = 0, \quad \text{for } \alpha = D, I, \quad (3.7)$$

$$k_o^D(s_o) < k_o^I(s_o), \quad \text{for } 0 < s_o < 1, \quad (3.8)$$

$$\frac{dk_o^\alpha}{ds_o} > 0 \quad \text{and} \quad \frac{d^2 k_o^\alpha}{ds_o^2} > 0, \quad \text{for } s_o \in (0, 1) \text{ and } \alpha = D, I. \quad (3.9)$$

Hypothesis (3.8) is true for most reservoirs. One physical mechanism to explain it is related to the change in the angle made by microscopic oil/water interface at pore walls when flow reverses between imbibition and drainage. We also assume that the scanning curves foliate the scanning region as π varies and that the graphs of the oil permeability functions in the scanning region are

smooth and intersect the graphs of the imbibition and drainage oil permeability functions transversally:

$$s_o^\alpha(0) = 0, \quad s_o^\alpha(1) = 1, \quad \text{for } \alpha = D, I, \quad (3.10)$$

$$k_o^S \in \mathcal{C}^2(\mathcal{S}), \quad (3.11)$$

$$k_o^S > 0, \quad \text{and} \quad \frac{\partial k_o^S}{\partial \pi} > 0, \quad \text{in } \mathcal{S}, \quad (3.12)$$

$$\frac{\partial k_o^S}{\partial s_o} > 0, \quad \text{and} \quad \frac{\partial^2 k_o^S}{\partial s_o^2} > 0, \quad \text{in } \mathcal{S}, \quad (3.13)$$

$$\frac{\partial k_o^S}{\partial s_o}(s_o^\alpha(\pi); \pi) < \frac{dk_o^\alpha}{ds_o}(s_o^\alpha(\pi)) \quad \text{for } \pi \in (0, 1), \text{ and } \alpha = D, I. \quad (3.14)$$

The assumptions (3.14) guarantee that in the drainage and in the imbibition regimes we have $\frac{ds_o^\alpha}{d\pi} > 0$, for $\alpha = D, I$. This means that in the drainage and in the imbibition regimes the relations (3.3) and (3.5) also define (implicitly) $\pi = \pi^\alpha(s_o)$ for $\alpha = D, I$, respectively.

Finally we make the technical assumptions that

$$\frac{d^2 k_o^\alpha}{d s_o^2} < \frac{\partial^2 k_o^S}{\partial s_o^2}, \quad \frac{\partial^2 k_o^S}{\partial s_o \partial \pi} \geq 0, \quad \text{and} \quad \frac{\partial^2 k_o^S}{\partial \pi^2} \geq 0, \quad (3.15)$$

along the curves $s_o = s_o^\alpha(\pi)$, for $\alpha = D, I$. These assumptions simplify the geometry of the foliation and its relationship with the boundary of \mathcal{S} .

Calculations show that the assumptions in (3.15) imply that $\frac{\partial^2 \pi^\alpha}{\partial s_o^2} > 0$, for $\alpha = D, I$ and that the boundary curves of the domain \mathcal{S} have the form exhibited in Fig. 3.1.

In order to unify the nomenclature let us define the “global” oil permeability function in the domain \mathcal{S} :

$$k_o(s_o; \pi) = \begin{cases} k_o^S(s_o; \pi), & \text{if } \pi^D(s_o) < \pi < \pi^I(s_o) \quad (\text{scanning}), \\ k_o^D(s_o), & \text{if } \pi = \pi^D(s_o) \quad (\text{drainage}), \\ k_o^I(s_o), & \text{if } \pi = \pi^I(s_o) \quad (\text{imbibition}). \end{cases} \quad (3.16)$$

With this notation we have $\lambda_w(s_w) = k_w(s_w)/\mu_w$, $\lambda_g(s_g) = k_g(s_g)/\mu_g$ and $\lambda_o(s_o; \pi) = k_o(s_o; \pi)/\mu_o$. Thus the flow with hysteresis for three phases in porous media may be modeled by the 2-equation system (2.9), augmented in the scanning mode by one equation, or augmented in the drainage or in the imbibition modes by specific restrictions, as follows:

$$\begin{cases} \frac{\partial s_w}{\partial t} + \frac{\partial f_w(s_w, s_g; \pi)}{\partial x} = 0, \\ \frac{\partial s_g}{\partial t} + \frac{\partial f_g(s_w, s_g; \pi)}{\partial x} = 0, \end{cases} \quad (3.17)$$

$$\begin{cases} a) \frac{\partial \pi}{\partial t} = & \text{if } k_o(s_o; \pi) = k_o^S(s_o; \pi) & \text{(scanning),} \\ b) \pi = \pi^D(s_o), & \text{if } k_o(s_o; \pi) = k_o^D(s_o) \text{ and } \frac{\partial s_o}{\partial t} > 0 & \text{(drainage),} \\ c) \pi = \pi^I(s_o), & \text{if } k_o(s_o; \pi) = k_o^I(s_o) \text{ and } \frac{\partial s_o}{\partial t} < 0 & \text{(imbibition),} \end{cases} \quad (3.18)$$

where the flow functions f_w and f_g were defined in (2.4-2.5).

The state space for system (3.17 - 3.18) can be defined as

$$\Omega = \{(s_w, s_g; \pi) \in \mathbb{R}^3 \mid 0 \leq s_w \leq 1, 0 \leq s_g \leq 1, 0 \leq s_w + s_g \leq 1, \pi^D(1 - (s_w + s_g)) \leq \pi \leq \pi^I(1 - (s_w + s_g))\}. \quad (3.19)$$

4. The Extended Flow Functions

In the construction of the Riemann solution of system (3.17-3.18), besides the waves connecting two initial states in the same regime, scanning, imbibition or drainage, we have also to consider the possibility of connecting states in distinct regimes. This is done by considering the extended fractional flow function, introduced in [2] for two phase flow, which we reintroduce here for three phase flow. For reader convenience, they are described briefly in the Appendix.

To a fixed value of the hysteresis parameter $\pi = \tau$ in the interval $[0, 1]$, we associate the following piecewise smooth function, denoted by ψ_τ , the graph of which is represented in bold in Fig. 3.1 in $(s_o; \pi)$ space. We define:

$$\psi_\tau(s_o) = \begin{cases} \pi^I(s_o), & \text{if } 0 \leq s_o \leq s_o^I(\tau) & \text{(imbibition),} \\ \tau, & \text{if } s_o^I(\tau) < s_o < s_o^D(\tau) & \text{(scanning),} \\ \pi^D(s_o), & \text{if } s_o^D(\tau) \leq s_o \leq 1 & \text{(drainage).} \end{cases} \quad (4.1)$$

The τ -extended flow functions relative to the oil phase correspond to the restrictions of the standard flow functions, defined in Section 2, to the curve

$(s_o, \psi_\tau(s_o))$. For example, the τ -extended oil permeability function k_o^τ , represented in bold in Fig. 3.2 in $(s_o; k_o)$ space, is defined as:

$$k_o^\tau(s_o) = k_o(s_o, \psi_\tau(s_o)) = \begin{cases} k_o^I(s_o), & \text{if } 0 \leq s_o \leq s_o^I(\tau) & (\text{imbibition}), \\ k_o^S(s_o; \tau), & \text{if } s_o^I(\tau) < s_o < s_o^D(\tau) & (\text{scanning}), \\ k_o^D(s_o), & \text{if } s_o^D(\tau) \leq s_o \leq 1 & (\text{drainage}). \end{cases} \quad (4.2)$$

Similarly, we define the extended mobility of phase oil, $\lambda_o^\tau = k_o^\tau / \mu_o$ and the total extended mobility as $\lambda^\tau = \lambda_w + \lambda_g + \lambda_o^\tau$.

Finally, the τ -extended fractional flow functions are defined in terms of λ^τ as follows:

$$f_w^\tau = \frac{\lambda_w}{\lambda^\tau}, \quad f_g^\tau = \frac{\lambda_g}{\lambda^\tau}, \quad f_o^\tau = \frac{\lambda_o^\tau}{\lambda^\tau}. \quad (4.3)$$

In the particular case of two phase flow (for example, $s_g \equiv 0$, and $s \equiv s_w = 1 - s_o$), the extended fractional flow function $f_w^\tau(s)$ is represented in Fig. 7.1 of the Appendix. Notice that the fractional flow function f_w^τ is piecewise smooth and consists of three portions: drainage, scanning and imbibition, represented in bold in Fig. 7.1 by f^D , f^S and f^I , respectively. The construction of the Riemann problem for two phase flow also is shown in the Appendix.

5. The Simple Model

We construct a simple three phase model with hysteresis, whose Riemann solution is easily described. From now on we use the notation u for water saturation and v for gas saturation. Let us define $z = u + v$. With this notation the oil saturation is $s_o = 1 - z$. We also define the functions $z^D(\pi) = 1 - s_o^D(\pi)$, $z^I(\pi) = 1 - s_o^I(\pi)$. In the simple model, defined by equation (5.1), we will assume that water and gas are miscible; that is, we will make use of linear relative permeability functions for water and gas, $k_w(u) = u$, $k_g(v) = v$, respectively, with corresponding viscosity $\mu_w = \mu_g$. Without loss of generality, the common value $\mu_w = \mu_g$ can be set to 1. Thus the mobilities are

$$\lambda_w(u) = u, \quad \lambda_g(v) = v, \quad \lambda_o(z; \pi) = \mu k_o(1 - z; \pi), \quad (5.1)$$

where $0 < \mu \leq 1$ is the gas-oil viscosity ratio and k_o is defined in (3.16), under the assumptions (3.6-3.15).

Notice that the total mobility λ , defined by equation (2.4), depends on z and π only. Thus for simplicity, we define the function

$$k(z; \pi) = k_o(1 - z; \pi), \quad (5.2)$$

we write

$$\lambda = \lambda(z; \pi) = z + \mu k(z; \pi), \quad (5.3)$$

and we introduce

$$q = \lambda^{-1}. \quad (5.4)$$

The relations in (3.17-3.18) may be written as

$$\begin{cases} u_t + (uq)_x = 0 \\ v_t + (vq)_x = 0 \end{cases} \quad (5.5)$$

$$\begin{cases} a) \frac{\partial \pi}{\partial t} = 0 & \text{(scanning),} \\ b) \pi = \pi^D(1 - z) \text{ and } \frac{\partial z}{\partial t} < 0 & \text{(drainage),} \\ c) \pi = \pi^I(1 - z) \text{ and } \frac{\partial z}{\partial t} > 0 & \text{(imbibition).} \end{cases} \quad (5.6)$$

5.1. The waves in the scanning regime. In the scanning regime the three phase flow for the simple hysteresis model is governed by equations (5.5-5.6a).

Let us begin our analysis by taking π to be constant. Thus on this plane with constant π in Ω the system (5.5-5.6a) reduces to the system (5.5), which means that two of the three characteristic speeds of the complete system (5.5-5.6a) are the characteristic speeds of system (5.5). It is well known [9] that for each constant π the system (5.5) possesses a linearly degenerate characteristic field with speed $a_c = q$, which corresponds to contact discontinuities in the Riemann solution of (5.5), with associated characteristic field $r_c = (q_v, -q_u, 0)^T$. We call the contact waves c -waves. Also, the other characteristic speed is $a_z = q + uq_u + vq_v$, which is associated to the characteristic field $r_z = (u, v, 0)^T$. We call the waves associated to this characteristic field z -waves.

The orbits of the z -waves in the scanning regime may be parameterized by z , taking a constant π and a constant θ such that

$$\begin{aligned} u &= z \cos \theta / (\cos \theta + \sin \theta), \\ v &= z \sin \theta / (\cos \theta + \sin \theta). \end{aligned} \quad (5.7)$$

Then along the orbits of the z -waves the equations in (5.5-5.6a) reduce to the following scalar conservation law

$$z_t + f(z; \pi)_x = 0, \quad (5.8)$$

where

$$f(z; \pi) = zq(z; \pi). \quad (5.9)$$

Thus, the z -waves may be obtained as solutions of the scalar equation (5.8) with flux function given by (5.9). Such z -waves are obtained as in Buckley-Leverett solution by using Oleinik's construction, with z restricted to the interval $(z^D(\pi), z^I(\pi))$, for each constant π .

Remark 1. We call $z \in [0, 1]$ the “equivalent saturation”. Denoting the z -derivative by the superscript “prime” we have that $q_u = q_v = q'$, and we can write for $z > 0$ and any π in the closure of the scanning region.

$$a_c(z; \pi) = f(z; \pi) / z, \quad r_c(z; \pi) = (1, -1, 0)^T, \quad (5.10)$$

$$a_z(z; \pi) = f'(z; \pi), \quad r_z(z; \pi) = (u, v, 0)^T. \quad (5.11)$$

Notice that $\lim_{z \rightarrow 0} a_c(z; \pi)$ exists; it allows us to define $a_z(0; \pi)$.

From (5.10), we obtain that the orbits of the c -waves (contact waves) are straight lines with constant π and constant z in Ω , along which a_c is constant.

Now let us take into account the variation of the parameter π in equations (5.5-5.6a). Condition (5.6.a), in the scanning mode, gives rise to a stationary contact wave in the Riemann solution, which was discussed in [2, 3, 4]. We have:

Lemma 5.1. *In the scanning region, the system (5.5-5.6a) possesses a stationary contact wave. The orbits for such stationary waves are contained in planes with constant θ in Ω . They are curves along which $f(z; \pi)$ is constant.*

Proof: The Rankine-Hugoniot condition for equation (5.6.a) yields the existence of the stationary wave. Substituting this zero shock speed in the Rankine-Hugoniot condition for (5.5) we obtain that the associated orbits are contained in planes with constant θ . Finally, restricting (5.5) to planes with constant θ , as in (5.7), and rewriting the Rankine-Hugoniot condition for equation (5.8) we obtain that $f(z; \pi)$ is constant. □

Remark 2. *(Implications for the construction of Riemann solutions). Summarizing the results of this subsection, the orbits of the characteristic fields in the scanning regime, given by system (5.5-5.6a), consist (i) of segments of straight lines with constant z (i.e. constant equivalent saturation) and constant π , along which the characteristic speed a_c (in (5.10)) is constant; (ii) of segments of straight lines through the origin with constant θ , and constant π , along which the equivalent saturation varies, the equations in (5.8), (5.9) are satisfied and the characteristic speed is a_z (in (5.11)); and (iii) of curves with constant θ along which $f(z; \pi)$ is constant and the characteristic speed is zero.*

5.2. Wave resonance in the scanning regime. To solve the Riemann problem for system (5.5-5.6a), we have to compare wave speeds associated to the three distinct characteristic fields.

Lemma 5.2. *Assume $\pi \in (0, 1)$ and $z \in (z^D(\pi), z^I(\pi))$. There are neither resonances between stationary waves and z -waves nor between stationary waves and c -waves. The z -waves and the c -waves are resonant at the straight line $\{z = z_c; \pi = \pi_c\}$, if and only if,*

$$k'(z_c; \pi_c) = -\mu^{-1} \quad (5.12)$$

Proof: Because $\frac{\partial k_z^s}{\partial s_0} > 0$ (see 3.13) we have that $k' < 0$ for $z \in (z^D(\pi), z^I(\pi))$. A direct calculation in (5.11) yields $a_z = \frac{\mu(k - zk')}{(z + \mu k)^2}$. Since $z > 0$, the function k is positive and $\mu k'$ is negative, within the scanning region we have $a_z > 0$. This implies that there is no resonance between stationary waves and z -waves. Similarly, since $\mu k > 0$ we have that $a_c = q = (z + \mu k)^{-1} > 0$, and again there is no resonance between stationary waves and c -waves within the scanning region. Finally, equating a_z to a_c , we complete the proof. \square

Now let us consider the final possibility of resonance in the scanning regime, between z -shocks and c -waves.

Lemma 5.3. *Let π and θ be constant and $z \in (z^D(\pi), z^I(\pi))$. For equation (5.8) with f given by (5.9), consider a shock between $(z_L, \theta; \pi)$ and $(z_R, \theta; \pi)$ with shock speed σ . There are two possibilities. Either the shock speed coincides with neither contact speed at sides $(z_L, \theta; \pi)$ and $(z_R, \theta; \pi)$, or else the shock speed coincides with the contact speeds at both sides $(z_L, \theta; \pi)$ and $(z_R, \theta; \pi)$, that is*

$$\sigma = \frac{f(z_L; \pi)}{z_L} = \frac{f(z_R; \pi)}{z_R}. \quad (5.13)$$

In the latter case, the coincidence in the $(z, \theta; \pi)$ space occurs along two straight lines on the plane with constant π . They are defined by $z = z_L$ and $z = z_R$, respectively.

Proof: The shock speed for (5.8) is

$$\sigma = \frac{f(z; \pi) - f(z_L; \pi)}{z - z_L} \quad (5.14)$$

Equating σ to a_c in Eq. (5.10) we conclude (5.13). \square

Remark 3. *(Implications for the construction of Riemann solutions). Equation (5.13) says that for each value of π , the coincidence of shock speeds σ (given*

by slopes of secants) with contact speeds (given by slopes of lines through the origin) can be found by plotting the graph of the function f given in (5.9) in the plane (z, f) . The double coincidence given by Eq. (5.13) locates changes from z -waves (lines in $(u, v; \pi)$ space through the origin of the plane with constant π) to c -waves (lines in $(u, v; \pi)$ space parallel to the hypotenuse of the saturation triangle on the plane with constant π).

5.3. The waves in the drainage and in the imbibition regimes. When the fluid movement is restricted to a drainage (with $\frac{\partial s_0}{\partial t} > 0$) or to an imbibition regime (with $\frac{\partial s_0}{\partial t} < 0$), we call it a “pure” regime. In such a case the flow with hysteresis is modeled by the system in (5.5) together the restrictions in (5.6b) in the drainage regime or (5.6c) in the imbibition regime.

The main difference between the scanning regime and a pure drainage or imbibition regime is that in the scanning regime there are stationary waves as consequence of equation (5.6a), while in a pure regime there are only c -waves and z -waves, since equation (5.6a) is replaced by relations (5.6b) or (5.6c). Thus the results of subsections (5.1-5.2), such as Remark 1, Lemma 5.2 and Lemma 5.3, relative to the characteristic speeds a_c and a_z are maintained, with the restrictions $\pi = \pi^\alpha(1 - z)$, $\alpha = D, I$.

We omit the proofs in this subsection and in the next ones, because they that are similar to those in the subsections (5.1) and (5.2).

For (z, θ, π) in a pure regime we have $a_c(z; \pi) = f(z; \pi^\alpha(1 - z)) / z$, $\alpha = D, I$, and since the first two components of $r_c(z; \pi)$ in (5.10) reflect the fact that the orbits of the c -waves lie on planes with constant z in (z, θ, π) space, it follows that $\pi^\alpha(1 - z)$ is constant and the third component of $r_c(z; \pi)$ is also zero. Thus, in a pure regime too the orbits of the c -waves consist of straight lines parallel to the hypotenuse of the saturation triangle with constant π . The other characteristic speed is $a_z(z; \pi) = f'(z; \pi^\alpha(1 - z))$. The first two components of r_z are the same as in (5.11), but the third component is not zero, because $\pi^\alpha(1 - z)$ varies with z along the orbits of r_z . Thus the orbits of the z -waves in a pure regime consist of curves with constant θ along the surface $\pi = \pi^\alpha(1 - z)$

with $\alpha = D, I$. The z -waves also may be obtained as solutions of equation (5.8), with f given in (5.9).

5.4. Wave resonance in a pure regime. The version of Lemmas (5.2) and (5.3) for a pure regime are given in Lemmas (5.4) and (5.5), which follow.

Lemma 5.4. *Consider flow in a pure regime. Then z -rarefactions and the c -waves are resonant at a straight line $\{z = z_c; \pi = \pi_c\}$, if and only if,*

$$k'(z_c; \pi_c) = -\mu^{-1}, \quad (5.15)$$

where $\pi_c = \pi^\alpha(1 - z_c)$, $\alpha = D, I$ for drainage or imbibition regime, respectively.

Remark 4. *We will assume in this work that in each pure regime equation (5.15) possesses exactly one solution z_c . This means that in each pure regime there is a straight line where the c -waves and the z -rarefaction are resonant. See Fig. 5.1 with $z_c = z_{C^I}$, corresponding to a resonance in the imbibition regime.*

Lemma 5.5. *Consider flow in a pure regime α (where $\alpha = D$ or $\alpha = I$, for drainage or imbibition, respectively) and θ constant. Consider the states $(z_L, \theta; \pi_L)$ and $(z_R, \theta; \pi_R)$ with $\pi_L = \pi^\alpha(1 - z_L)$ and $\pi_R = \pi^\alpha(1 - z_R)$. Consider a shock for equation (5.8) with $f = f(z; \pi^\alpha(1 - z))$ given by (5.9) between $(z_L, \theta; \pi_L)$ and $(z_R, \theta; \pi_R)$ with associated shock speed σ . There are two possibilities. Either the shock speed coincides with neither contact speed at sides $(z_L, \theta; \pi_L)$ and $(z_R, \theta; \pi_R)$, or else the shock speed coincides with the contact speeds at both sides $(z_L, \theta; \pi_L)$ and $(z_R, \theta; \pi_R)$, that is*

$$\sigma = \frac{f(z_L; \pi_L)}{z_L} = \frac{f(z_R; \pi_R)}{z_R}. \quad (5.16)$$

In the latter case, the coincidence in $(z, \theta; \pi)$ space occurs along the two straight lines $\{z = z_L, \pi = \pi^\alpha(1 - z_L)\}$ and $\{z = z_R, \pi = \pi^\alpha(1 - z_R)\}$.

5.5. Waves connecting distinct regimes. In the previous subsections we discussed the waves and their coincidence when the fluid flow is restricted to the scanning, or to the drainage, or to the imbibition regimes. Now we discuss the possibility of waves connecting states in distinct regimes. To do so, we will make use of the concept of extended flow functions, introduced in Section 4.

Because we use the variable $z = 1 - s_o$ here, we redefine the extended functions in the variable z . We have:

$$\phi_\tau(z) \equiv \psi_\tau(1 - z) = \begin{cases} \pi^D(1 - z), & \text{if } 0 \leq z \leq z^D(\tau) & (\text{drainage}), \\ \tau, & \text{if } z^D(\tau) < z < z^I(\tau) & (\text{scanning}), \\ \pi^I(1 - z), & \text{if } z^I(\tau) \leq z \leq 1 & (\text{imbibition}). \end{cases} \quad (5.17)$$

The τ -extended oil permeability function $k^\tau(z)$ is defined as:

$$k^\tau(z) = k(z; \phi_\tau(z)) \quad (5.18)$$

Similarly, the τ -extended fractional flow function for equation (5.8) is defined in terms of $k^\tau(z)$ as follows:

$$f^\tau(z) = f(z; \phi_\tau(z)) = \frac{z}{z + \mu k^\tau(z)} \quad (5.19)$$

The graph of function f^τ is represented in Fig. 5.1 in bold.

Remark 5. According to assumptions in (3.10), if $\tau = 0$ then $z^D(0) = z^I(0) = 1$ and f^0 coincides with the drainage flow function f^D , since $k^0 \equiv k^D$. If $\tau = 1$ then $z^D(1) = z^I(1) = 0$ and f^1 coincides with the imbibition flow function f^I , since $k^1 \equiv k^I$. If $\tau \in (0, 1)$, then from assumptions (3.6 - 3.14) f^τ is piecewise smooth with finite lateral z -derivative at the joining points $z^D(\tau)$ and $z^I(\tau)$.

From the Remark 5 above, the functions $a_c(z; \phi_\tau(z))$ and $r_c(z; \phi_\tau(z))$ are continuous when the fluid flow changes from one regime to the other, but a_z and r_z are only piecewise continuous, since they depend on the z -derivative.

The resonances between the speeds a_z and a_c restricted to the curve $(z; \phi_\tau(z))$ must be considered for z in each of the disjoint intervals $[0, z^D(\tau)]$, $(z^D(\tau), z^I(\tau))$ and $[z^I(\tau), 1]$. In each interval, the resonances behave as in Lemmas 5.2 and 5.4, but at the points $z^D(\tau)$ and $z^I(\tau)$ the lateral z -derivatives must be considered.

The results of Lemmas 5.3 and 5.5 about coincidence of shock speeds are also maintained, but we may have left states and right states in distinct regimes. We have:

Lemma 5.6. *Consider a fixed $\tau \in [0, 1]$ and a constant θ . Consider $(z_L, \theta; \pi_L)$ and $(z_R, \theta; \pi_R)$ such that $\pi_L = \phi_\tau(z_L)$ and $\pi_R = \phi_\tau(z_R)$. Consider a shock for equation (5.8) with f given by f^τ in (5.19), between $(z_L, \theta; \pi_L)$ and $(z_R, \theta; \pi_R)$ with associated shock speed σ . There are two possibilities. Either the shock speed coincides with neither contact speed at sides $(z_L, \theta; \pi_L)$ and $(z_R, \theta; \pi_R)$, or else the shock speed coincides with the contact speeds at both sides $(z_L, \theta; \pi_L)$ and $(z_R, \theta; \pi_R)$, that is*

$$\sigma = \frac{f^\tau(z_L)}{z_L} = \frac{f^\tau(z_R)}{z_R}. \quad (5.20)$$

In the latter case, the coincidence in the $(u, v; \pi)$ space occurs along the two straight lines $\{z = z_L, \pi = \phi_\tau(z_L)\}$ and $\{z = z_R, \pi = \phi_\tau(z_R)\}$.

From (3.9), (3.13) and (3.14) it is easy to see that there are no resonances between imbibition or drainage rarefaction waves with scanning rarefaction waves, nor with stationary waves.

Remark 6. *Since the graph of the function f^τ possesses two points with discontinuous derivative, there may exist a triple coincidence of shock speeds, as shown in Fig. 5.2 with $z_L = z_L^D$ and $z_L = z_L^I$.*

Remark 7. *(Implications for the construction of Riemann solutions). Equation (5.20) says that for each value of τ , the coincidence of shock speeds σ (given by slopes of secants) with contact speeds (given by slopes of lines through the origin) can be found by plotting the graph of the function f^τ given in (5.19) in the plane (z, f^τ) . The double coincidence given by Eq. (5.20) locates changes from z -waves (curves in $(u, v; \pi)$ space along planes with constant θ) to c -waves (lines in $(u, v; \pi)$ parallel to the hypotenuse of the saturation triangle).*

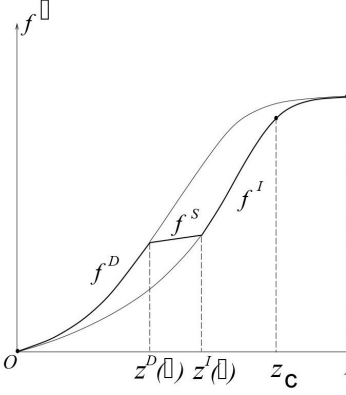


Figure 5.1: The τ extended flow function.

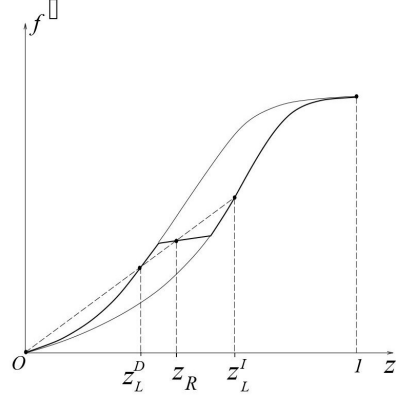


Figure 5.2: Triple coincidence of shocks.

6. The Riemann solution

6.1. Preliminaries. In order to reduce the complexity of the example of Riemann solution to be described in the Subsection 6.3, we make some simplifying assumptions.

First off all, we assume that the problem to be solved has weak drainage-imbibition hysteresis strength, which means that for each value of the parameter π we have that s_o varies in a small interval $(s_o^I(\pi), (s_o^D(\pi))$.

Second, we assume that: $\frac{\partial k^S}{\partial s_o} < \frac{1}{\mu}$ for $(s_o; \pi) \in \mathcal{S}$. One of the consequences is that the equation (5.12) does not possess any solution, which means that there are no resonances in the scanning regime. Consequently there is no generic scanning shock with speed coinciding with a contact speed analogous to Eq. (5.13), for any value of π .

Third, just to simplify the description of the Riemann solution, for each value of $\pi = \tau$ we assume that the graph portion of the function f^τ corresponding to z in the interval $(z^D(\tau), z^I(\tau))$ is a straight line segment (with slope a_z less

than a_c). This means that the scanning z -waves will also be contact waves in this work. In this way, we avoid some technicalities in analyzing the internal structure of the scanning waves.

In general, each level set with constant π defines a two dimensional scanning leaf of the scanning foliation in $(u, v; \pi)$ space. We call this surface a *scanning surface*. For the simple model each leaf is a surface ruled by lines with constant z and in particular, under the third simplifying assumption the scanning surface reduces to a planar surface.

We recall that according to the Remarks and Lemmas of subsections 5.1-5.5 the fundamental waves in the Riemann solution are stationary waves, z -waves and c -waves. As we saw in the proof of the Lemma 5.2 for the scanning regime the speeds of z -waves and c -waves are positive. An analogous proof for the drainage and imbibition regimes shows that the wave speeds a_c and a_z are positive, except for the extremities $z = 0$ and $z = 1$. Thus, given a left state $L \equiv (u_L, v_L, \pi_L) \equiv (z_L, \theta_L; \pi_L)$ generically the first wave in the Riemann solution from state L to a state $R \equiv (u_R, v_R; \pi_R) \equiv (z_R, \theta_R; \pi_R)$ is a stationary wave.

If R lies on the orbit of the characteristic field associated to the stationary wave through L , then the Riemann solution is complete and consists only of the stationary wave. In this case, according to Lemma 5.1, we must have $\theta_R = \theta_L$ and $f(z_R; \pi_R) = f(z_L; \pi_L)$.

If R does not belong to the orbit associated to the stationary wave through L , then the c -waves and z -waves may be present in the Riemann solution, after a constant state M on the stationary wave through L . Thus we have to consider a two dimensional surface in state space Ω consisting of intermediate states M such that the Riemann problem with generic left state M and right state R is solved by a sequence of c -waves and z -waves under the compatibility condition that wave speed must increase from left to right in the physical space (x, t) . We call this surface the M -surface associated to R , or only the M -surface, when it is clear which R is being considered.

Once we have obtained the M -surface associated to R , because of transver-

salinity between the stationary orbit and the M -surface, the Riemann problem with left state L and right state R may be solved uniquely by determining the intermediate state M defined by the intersection of the stationary orbit through L with the M -surface.

6.2. The R -regions. The states R for which the wave structure and topology of the M -surface are similar are lumped into an R -region. From the Remarks 2, 3 and 7 the orbits of the c -waves consist of straight lines with constant z and constant π , but the orbits of the z -waves depend on π and z and lie along planes with constant θ . It turns out that it is more convenient to represent the R -regions in (z, f^τ) variables. Each point in (z, f^τ) space corresponds to a straight line segment in $(u, v; \pi)$ space for which $u + v = z = \text{constant}$ and $\pi = \text{constant}$, and each curve corresponds to a surface ruled by such straight lines. Each section $\theta = \text{constant}$ of the state space boundary is given by $\pi = \pi^D(1 - z)$ and $\pi = \pi^I(1 - z)$; one such section is shown in Fig. 3.1 in the $(s_o; \pi)$ space and corresponds in the (z, f^τ) space to the graph of the drainage flow function $f^D \equiv f^0$ and to the graph of the imbibition flow function $f^I \equiv f^1$, respectively, shown in Fig. 5.1.

For this problem, there are 3 disjoint R -regions, represented in Fig. 6.1 as $Scan(1)$, $Scan(12)$ and $Scan(2)$. The regions $Scan(1)$ and $Scan(2)$ are volumes. They are separated by the ruled surface $Scan(12)$. This surface $Scan(12)$, represented in Fig. 6.1 as the segment of the straight line tangent to the point C^I (which continuation through the origin is not drawn), is defined as the set of states R in state space Ω such that $a_c(z_R; \pi_R) = a_z(z_c; \pi^I(1 - z_c))$, where z_c is the z -coordinate of point C^I . The point C^I in Fig. 6.1 corresponds to the resonant straight line $\{z = z_c; \pi = \pi^I(1 - z_c)\}$ established in Lemma 5.4 and in Remark 4 for the imbibition regime.

We also represent in Fig. 6.1 the boundary surfaces $Drain(1)$ and $Imb(1)$ of the R -region $Scan(1)$ and the boundary surfaces $Drain(2)$, $Drain(2')$, and $Imb(2)$ of the R -region $Scan(2)$. They correspond to the pure regimes, drainage or imbibition, for the right state R . The boundary between $Drain(2)$

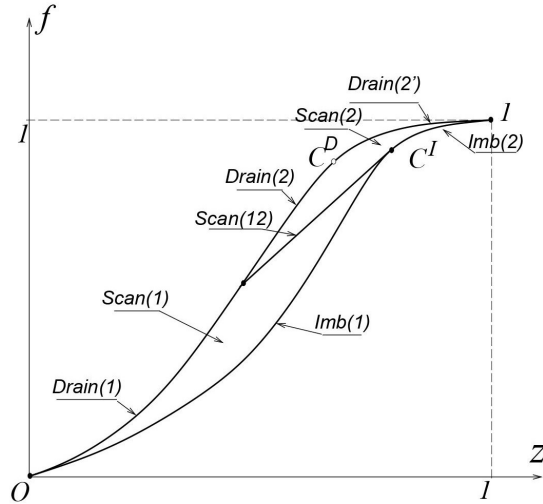


Figure 6.1: R -Regions for the Riemann solution.

and $Drain(2')$ is defined by the resonant straight line $\{z = z_{C^D}, \pi = \pi^D(1 - z_{C^D})\}$ while the boundary between $Imb(1)$ and $Imb(2)$ is defined by the resonant straight line $\{z = z_{C^I}, \pi = \pi^I(1 - z_{C^I})\}$, as established in Lemma 5.4.

Remark 8. *The relative size of a_c and a_z in the three R -regions and their boundaries shown in Fig. 6.1 is the following (the relationship is based on assumptions (3.6-3.14) and on the equations (5.3), (5.4), (5.9), (5.10), (5.11) and on the simplifying assumptions considered in the Subsection .*

In $Scan(1)$, $Scan(12)$, $Scan(2)$, $Imb(2)$ and $Drain(2')$, $a_c > a_z$.

In $Imb(1)$, $Drain(1)$ and $Drain(2)$, $a_c < a_z$.

6.3. The construction of the M -surfaces. Let $R \equiv (u_R, v_R; \pi_R) \equiv (z_R, \theta_R; \pi_R)$ in the R -region $Scan(1)$.

In order to describe the sequence of c -waves and z -waves that define the

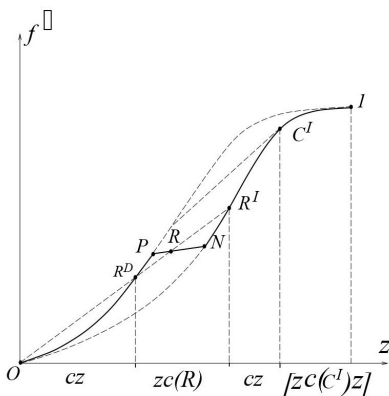


Figure 6.2: Construction of the M -surface for $R \in \text{Scan}(1)$, represented in (z, f^τ) space.

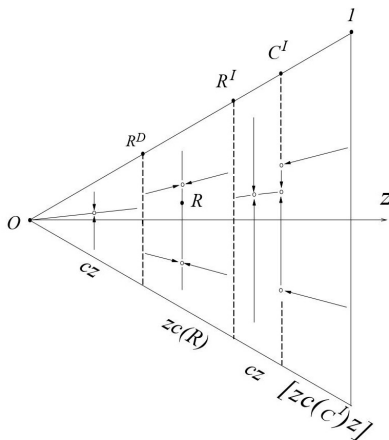


Figure 6.3: Projection of the M -surface for $R \in \text{Scan}(1)$ in saturation triangle $\pi = \pi_R$.

M -surface consider the τ -extended fractional flow function with $\tau = \pi_R$, denoted here by f^R . The graph of the extended flow function f^R is represented in bold in Fig. 6.2 as the curve $[0PRN1]$. As θ varies the portion $[0, P]$ corresponds to states in Ω in the drainage regime; the portion (PRN) corresponds to states in the scanning regime and the portion $[N1]$ corresponds to states in the imbibition regime.

In order to determine all sequences of waves connecting M in the M -surface to R , we have to compare the speeds of c -waves (given by slopes of straight lines through the origin and through a state on the curve $[0PRN1]$ in Fig. 6.2), with speeds of z -waves (given by the slope a_z in each segment $[0P]$, (PRN) or $[N1]$ of the graph of f^R). To do so, consider the straight line with slope given by $a_c(R) = f^R(z_R) / z_R$ through the origin 0 and through the state R in Fig. 6.2. Since $a_z(R) < a_c(R)$, this line crosses the drainage portion $[0P]$ and crosses the

imbibition portion $[N1]$. These intersections define the points R^D and R^I in Fig. 6.2, respectively. The z -coordinates of R^D , R^I and C^I are denoted by z_{R^D} , z_{R^I} and z_{C^I} , respectively. The states R^D and R^I in Fig. 6.2 correspond to the states with z -coordinates z_L^D and z_L^I in Fig. 5.2 established in Lemma 5.6 and Remark 6, where contact speeds and z -shock speeds coincide.

According to Lemma 5.5, another change in speed order may occur at the point C^I of Fig. 6.2, where there is a coincidence between the speeds a_z and a_c in the imbibition regime.

Thus the graph of the extended flow function f^R is divided into four disjoint portions represented in bold in Fig. 6.2 as $[0R^D]$, $[R^D R^I]$, $[R^I C^I]$ and $[C^I 1]$.

Lemma 6.1. *The M -surface for any state R in R -region $\text{Scan}(1)$ is a ruled surface, which is piecewise smooth, and consists of four components corresponding to the portions $[0R^D]$, $[R^D R^I]$, $[R^I C^I]$ and $[C^I 1]$ of the graph of f^R in Fig. 6.2. The sequence of waves connecting an intermediate state $M = (z_M, \theta_M; \pi_M)$ to the state R is defined in terms of the coordinate z_M as follows:*

- (a) For $0 \leq z_M \leq z_{R^D}$, the sequence is: $(z_M, \theta_M; \pi_M) \xrightarrow{c} (z_M, \theta_R; \pi_M) \xrightarrow{z} (z_R, \theta_R; \pi_R)$, denoted by cz in Figs. 6.2 and 6.3;
- (b) For $z_{R^D} \leq z_M \leq z_{R^I}$, the sequence is: $(z_M, \theta_M; \pi_M) \xrightarrow{z} (z_R, \theta_M; \pi_R) \xrightarrow{c} (z_R, \theta_R; \pi_R)$, denoted by $zc(R)$ in Figs. 6.2 and 6.3;
- (c) For $z_{R^I} \leq z_M \leq z_{C^I}$, the sequence is: $(z_M, \theta_M; \pi_M) \xrightarrow{c} (z_M, \theta_R; \pi_M) \xrightarrow{z} (z_R, \theta_R; \pi_R)$, also denoted by cz in Figs. 6.2 and 6.3;
- (d) For $z_{C^I} \leq z_M \leq 1$, the sequence is:
 $(z_M, \theta_M; \pi_M) \xrightarrow{z} (z_{C^I}, \theta_M; \pi_{C^I}) \xrightarrow{c} (z_{C^I}, \theta_R; \pi_{C^I}) \xrightarrow{z} (z_R, \theta_R; \pi_R)$, denoted by $[zc(C^I)z]$ in Figs. 6.2 and 6.3, where $\pi_{C^I} = \pi^I(1 - z_{C^I})$.

Proof: (a) Since $0 \leq z_M \leq z_{R^D}$ the state M belongs to the component of the M -surface corresponding to the portion $[0R^D]$ in Fig. 6.2 and $a_c(M) \leq a_z(M)$.

Thus, consider the c -contact orbit through the state M , given by the straight line $\{z = z_M; \pi = \pi_M\}$ (see Fig. 6.3).

Consider the state \tilde{M} , the intersection of this c -orbit with the plane $\theta = \theta_R$. The speed of the c -wave connecting M to \tilde{M} is $a_c(M) = a_c(\tilde{M}) = f^R(z_M) / z_M$. Now, following Oleinik's construction, consider the z -shock wave connecting \tilde{M} to R with speed σ . As we know \tilde{M} corresponds to a point on the graph of f^R in the segment $[0R^D]$ in Fig. 6.2. Since the secant to the graph of f^R joining any state in the segment $[0R^D]$ to R has slope larger than $a_c(\tilde{M})$, the shock speed σ is larger than the contact speed $a_c(\tilde{M})$. Thus the state M can be connected to the state R by a contact wave followed by a z -shock wave, which proves item (a).

(b) The state M belongs to the component of the M -surface corresponding to the portion $[R^D R^I]$ of the graph of f^R in Fig. 6.2. Thus we have $a_c(M) \equiv f^R(z_M) / z_M \geq [f^R(z_R) - f^R(z_M)] / [z_R - z_M]$. Thus consider the c -orbit through R , which is the straight line given by $\{z = z_R; \pi = \pi_R\}$ drawn in Fig. 6.3. Let \tilde{M} be the state defined by the intersection of this c -orbit with the plane $\theta = \theta_M$. Now consider Oleinik's construction for equation (5.8) with $f = f^R$ in the plane $\theta = \theta_M$, with left state $(z_M; \pi_M)$ and right state $(z_R; \pi_R)$. If M is either a state in the drainage regime corresponding to a point in the portion $[R^D P]$ or a state in the imbibition regime corresponding to a point in the portion $[NR^I]$ of the graph f^R in Fig. 6.2, then the z -wave is a shock wave with speed $(f^R(z_R) - f^R(z_M)) / (z_R - z_M)$; if M is a state in the scanning regime corresponding to a point in the portion $[PN]$ of the graph f^R , then the z -wave is a contact wave with speed $a_z(M) = a_z(R)$. In both cases the speed of the c -wave connecting \tilde{M} to R is larger than the speed of the z -wave connecting M to \tilde{M} and item (b) is proved.

(c) The state M belongs to the component of the M -surface corresponding to the portion $[R^I C^I]$ of the graph f^R in Fig. 6.2. Thus $a_c(M) \leq a_z(M)$ and the sequence of waves is the same as that obtained in item (a).

(d) The state M belongs to the component of the M -surface corresponding to the portion $[C^I 1]$ of the graph of f^R in Fig. 6.2. We have $a_c(M) \geq a_z(M)$. Thus

the first wave connecting M to R is a z -wave. By Oleinik's construction for equation (5.8) with f given by f^R in the plane $\theta = \theta_M$, with left state $(z_M; \pi_M)$ and right state $(z_R; \pi_R)$, this first wave is an imbibition rarefaction wave. Since the state C^I on the graph of f^R corresponds to a state $(z_{C^I}, \theta_M; \pi_{C^I})$, with $\pi_{C^I} = \pi^I(1 - z_{C^I})$, where the c -wave and the z -wave are resonant, it follows that the z -wave changes to a c -wave at this state. Thus, consider the c -orbit through the state $(z_{C^I}, \theta_M; \pi_{C^I})$, which is the straight line $\{z = z_{C^I}; \pi = \pi_{C^I}\}$ represented in Fig. 6.2 as the state C^I and in Fig. 6.3 as part of the vertical straight line through C^I . Consider the state defined by the intersection of this c -orbit with the plane $\theta = \theta_R$ given by $(z_{C^I}, \theta_R; \pi_{C^I})$ and represented by the same point C^I in Fig. 6.2. Since the speed a_c and the speed a_z coincide at $(z_{C^I}, \theta_R; \pi_{C^I})$, there is another change in wave order from the c -wave to the z -wave. Following Oleinik's construction for equation (5.8) with f given by f^R in the plane $\theta = \theta_R$, with left state $(z_{C^I}; \pi_{C^I})$ and right state $(z_R; \pi_R)$, this last z -wave is a "composite" wave consisting of an imbibition rarefaction wave followed by a scanning shock wave. This completes the proof of the Lemma. \square

Remark 9. *The sequence of waves in item (d) of Lemma 6.1 is only one wave with a single speed in physical space, represented in state space by four waves (an imbibition rarefaction, an imbibition contact, an imbibition rarefaction and a scanning shock) that propagate as a single object, without any intermediate state in physical space (x, t) separating the state M from the state R .*

The M -surface for right states R in the other R -regions and boundaries may be obtained as limit cases for R in $Scan(1)$ as follows.

If R moves from $Scan(1)$ to $Imb(1)$ the points R , N and R^I in Fig. 6.2 coincide. Similarly, if R moves from $Scan(1)$ to $Drain(1)$ the points R , P and R^D coincide. In both cases, the components of the M -surface remain

unchanged.

Case $R \in \text{Scan}(12)$.

If R moves from $\text{Scan}(1)$ to $\text{Scan}(12)$, according to the definition of surface $\text{Scan}(12)$ the points R^I and C^I in Fig. 6.2 coincide. In this case, the component of the M -surface defined by $[R^I, C^I]$ in Fig. 6.2 with wave sequence given in Lemma 6.1 c disappears. The other three components of the M -surface remain unchanged.

Case $R \in \text{Scan}(2)$.

If R moves from $\text{Scan}(12)$ to $\text{Scan}(2)$ the point C^I in Fig. 6.2 does not exist because the straight line through 0 and R does not intersect the portion $[N1]$ of the graph f^R any more. Thus the component of the M -surface defined by the portion $[C^I, 1]$ in Fig. 6.2 disappears, and we are left with only two components of the M -surface, defined by $[0, R^D]$ and $[R^D, 1]$ with wave sequences corresponding to items (a) and (b) of Lemma 6.1.

If R moves from $\text{Scan}(2)$ or from $\text{Imb}(1)$ to $\text{Imb}(2)$ the points R and N of Fig. 6.2 move over the point C^I and coincide. On the other hand, if R moves from $\text{Scan}(2)$ or from $\text{Drain}(1)$ to $\text{Drain}(2)$ the points R and P of Fig. 6.2 coincide. In both cases the M -surface possesses only two components with waves sequence corresponding to items (a) and (b) of Lemma 6.1, which are the same as in case $R \in \text{Scan}(2)$.

6.4. The transversality. As we said before, in order to complete the Riemann solution we have to establish the transversality between the stationary orbit (0-orbit) through L and the M -surface associated to R .

According to Lemma 5.1 the 0-orbits are curves with constant θ such that $f(z; \pi)$ is also constant as z and π vary. This means that the 0-orbit through L corresponds to a horizontal straight line through L in space $(z; f^\tau)$ in Fig. 6.2. Since $d f^R / d z = a_z > 0$ it follows that the horizontal straight line through state L will never be tangent to the graph of f^R projected on the plane $\theta = \theta_L$, which

means that the 0-orbit is transversal to the ruled M -surface.

Thus we have proved the following

Theorem 6.2. *For a given left state L and a given right state R in state space Ω , the Riemann solution for the simple model (5.5-5.6) exists and generically consists of a stationary wave connecting L to an intermediate state M followed by a sequence of c -waves and z -waves connecting M to R . The sequence is determined by with component of the M -surface the state M belongs to.*

Under the assumption that the two phase Riemann problem in the Appendix has a unique solution for each initial data, we believe that the arguments in this section could be used to establish the uniqueness of solution for each initial data, but we do not do it here.

7. Appendix - Solution of the Riemann Problem for the Two-Phase Flow Model

In this Appendix we obtain the Riemann solution for the two phase hysteresis model (water-oil). This solution was proposed in [3], [4], [5], and in [2]. The dependent variable is the water saturation $s \equiv s_w = 1 - s_o$. We will use notation introduced in Sections 3 and 4. We assume that the fractional flow functions, f^D and f^I , for the drainage and the imbibition regimes are \mathcal{C}^2 functions and possess only one inflection point, respectively, with

$$\begin{aligned} 0 < f^I(s) < f^D(s), \quad \text{for } s \in (0, 1), \\ f^I(0) &= f^D(0) = 0, \\ f^I(1) &= f^D(1) = 1. \end{aligned}$$

In this case the flow is modeled by the system

$$s_t + f(s; \pi)_x = 0 \quad (7.1)$$

$$\frac{\partial \pi}{\partial t} = 0 \quad (\text{scanning}), \quad (7.2)$$

$$\pi = \pi^D(1 - s) \quad \text{and} \quad \frac{\partial s}{\partial t} < 0 \quad (\text{drainage}), \quad (7.3)$$

$$\pi = \pi^I(1 - s) \quad \text{and} \quad \frac{\partial s}{\partial t} > 0 \quad (\text{imbibition}), \quad (7.4)$$

where

$$f(s; \pi) = \begin{cases} f^D(s), & \text{if } \pi = \pi^D(1 - s) & (\text{drainage}), \\ f^S(s; \pi), & \text{if } \pi^D(1 - s) \leq \pi \leq \pi^I(1 - s) & (\text{scanning}), \\ f^I(s), & \text{if } \pi = \pi^I(1 - s) & (\text{imbibition}), \end{cases} \quad (7.5)$$

is a continuous function, piecewise \mathcal{C}^2 and $f^S(s; \pi)$ is the scanning fractional flow function.

For a fixed value of $\pi = \tau \in (0, 1)$, the τ -extended fractional function (defined in Section 4) is given by

$$f^\tau(s) = \begin{cases} f^D(s), & \text{if } 0 \leq s \leq s^D(\tau), \\ f^S(s; \pi), & \text{if } s^D(\tau) < s < s^I(\tau), \\ f^I(s), & \text{if } s^I(\tau) \leq s \leq 1, \end{cases} \quad (7.6)$$

where $s^D(\tau)$ and $s^I(\tau)$ are implicitly defined by the first equation in (7.3) and (7.4), respectively.

In the scanning mode the characteristic speeds of system (7.1)-(7.2) are given by $a_0 = 0$ and $a_s = f_s$. The waves associated to a_0 are stationary waves (contact waves); the waves associated to a_s are called saturation waves.

From equation (7.2) it follows that the contact curves associated to a_0 (0-curves) are represented in space (s, f) , as horizontal straight lines, because the Hugoniot condition gives us that $f(s, \pi)$ is constant along such orbits.

Since $a_s = f_s > 0$ (for $s \neq 0$), for a given left state $u_L = (s_L; \pi_L)$ and a given right state $u_R = (s_R; \pi_R)$, the corresponding Riemann solution consists of the stationary wave connecting the state u_L to some intermediate state $u_M = (s_M; \pi_M)$, followed by a saturation wave connecting u_M to u_R . See Fig. 7.2.

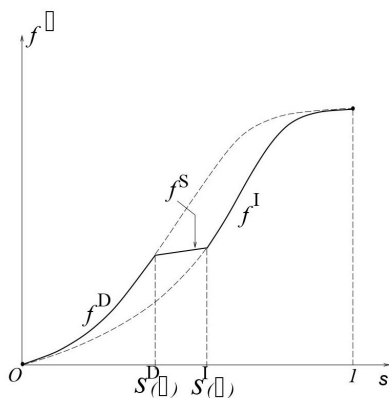


Figure 7.1: The τ extended flow function for the two phase flow.

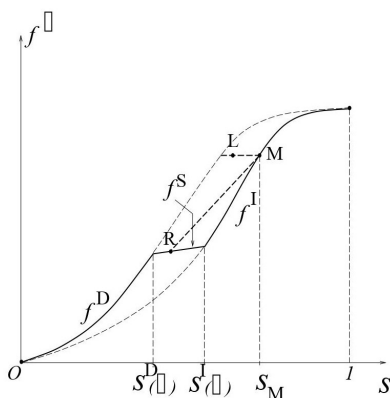


Figure 7.2: Illustration of the construction of the Riemann solution.

In order to determine the state u_M , we consider the τ -extended fractional function $f^\tau(s)$, with $\tau = \pi_R$, represented as a bold solid curve in Figs. 7.1 and 7.2.

In the space (s, f) , we identify the state u_L with the point $L = (s_L, f(s_L; \pi_L))$ and the state u_R with the point $R = (s_R, f^\tau(s_R))$. See Fig. 7.2 for a particular left state $(s_L; \pi_L)$.

Since the graph of f^τ is never horizontal ($f_s^\tau > 0$, for $s \neq 0$), the horizontal straight line through L , corresponding to the 0-orbit through u_L , crosses the graph of f^τ at some point that we define as $M = (s_M, f^\tau(s_M))$. For the particular state $(s_L; \pi_L)$, this orbit is represented as the bold horizontal dashed line through L in Fig. 7.2. This defines the coordinate s_M of the state u_M . The value of the component π_M depends on which segment of the graph of f^τ the

point M belongs to. We have

$$\pi_M = \pi^D(1 - s_M) \quad \text{for} \quad 0 \leq s_M \leq s^D(\tau); \quad (7.7)$$

$$\pi_M = \tau = \pi_R \quad \text{for} \quad s^D(\tau) \leq s_M \leq s^I(\tau); \quad (7.8)$$

$$\pi_M = \pi^D(1 - s_M) \quad \text{for} \quad s^I(\tau) \leq s_M \leq 1. \quad (7.9)$$

Once we have determined the state $u_M = (s_M; \pi_M)$, the saturation wave connecting u_M to u_R is determined by solving the Riemann problem with left state s_M and right state s_R , for the scalar conservation law

$$s_t + f^\tau(s)_x = 0, \quad (7.10)$$

by using a generalization of the Oleinik's envelope construction for the continuous piecewise smooth flux function $f^\tau(s)$. In Fig 7.2, such a Riemann solution is a shock wave connecting s_M to s_R . This shock is represented by the bold dashed line connecting the points M and R .

In this way we obtain the values of the water saturation s connecting s_M to s_R . The corresponding values of π connecting π_M to π_R , are obtained according to equations (7.2-7.4) and (7.7-7.9), that is, $\pi_M = \pi_R$, for $s^D(\pi_R) \leq s_M \leq s^I(\pi_R)$, or $\pi = \pi^\alpha(1 - s)$, $\alpha = D, I$, for s defined by the saturation wave connecting s_M to s_R .

Acknowledgement: We thank Beata Gundelach for the expert composition of the figures and text.

References

- [1] Aziz, A.; Settari, A., *Petroleum Reservoir Simulation*, Elsevier Applied Science, New York-London, (1990).
- [2] Bedrikovetsky, P.; Marchesin, D.; Ballin, P. R., *Mathematical Model for Immiscible Displacement Honouring Hysteresis*, SPE 30132, Fourth Latin American and Caribbean Petroleum Engineering Conference, Port of Spain, Trinidad-Tobago, (1996), 557-575.

- [3] Furati, Kh., *The Solution of the Riemann Problem for a Hyperbolic System Modeling Polymer Flooding with Hysteresis*, J. of Math. Anal. and Appl., vol. 206, (1997), 205-233.
- [4] Furati, Kh., *A Hysteretic Polymer Flooding Model*, Ph.D. Thesis, Duke University, Dept. of Mathematics, (1995).
- [5] Furati, Kh., *Effects of Relative permeability Hysteresis Dependence on Two-Phase Flow in Porous Media*, Transport in Porous Media, vol. 28, (1997), 181-203.
- [6] Marchesin, D.; Medeiros, H. B.; Paes-Leme, P. J., *A Model for Two Phase Flow with Hysteresis*, Contemporary Mathematics - A.M.S., vol. 60, (1987), 89-107.
- [7] Marchesin, D.; Medeiros, H. B.; Paes-Leme, P. J., (in memoriam), *Hysteresis in Two-Phase Flow: a Simple Mathematical Model*, Computational and Applied Mathematics, vol. 17, (1998), 81-99.
- [8] Peaceman, D., *Fundamentals of Numerical Reservoir Simulation*, Elsevier, Amsterdam, (1977).
- [9] Temple, B., *Systems of Conservation Laws with invariant submanifolds*, Trans. Math. Soc., vol. 280, n° 2, (1980), 781-795.

Universidade Federal da Paraíba
 Campina Grande, PB, Brazil
e-mail: cido@dme.ufpb.br

IMPA, Estrada Dona Castorina 110
 22460-320 Rio de Janeiro, RJ, Brazil
e-mail: marchesin@impa.br

UENF, Macaé, RJ, Brazil
e-mail: pavel@lenep.uenf.br

IMPA, Estrada Dona Castorina 110
 22460-320 Rio de Janeiro, RJ, Brazil
e-mail: krause@impa.br